



Technological University Dublin  
ARROW@TU Dublin

---

Articles

DIT Biophotonics and Imaging

---

2017-07-01

## Formulation, characterisation and stability assessment of a food derived 1 tripeptide, Leucine-Lysine-Proline loaded chitosan nanoparticles

M.K. Danish

*Technological University Dublin*

Giuliana Vozza


*Technological University Dublin*

Hugh Byrne

*Technological University Dublin, hugh.byrne@tudublin.ie*

Jesus Maria Frias

Follow this and additional works at: <https://arrow.tudublin.ie/biophonart>  
*Technological University Dublin, Jesus.Frias@tudublin.ie*

 Part of the [Food Biotechnology Commons](#), [Human and Clinical Nutrition Commons](#), [Medicinal-](#)

[Sinéad Ryan](#)  
[Pharmaceutical Chemistry Commons](#), and the [Physics Commons](#)  
*University College Dublin, Ireland*

---

### Recommended Citation

"Formulation, characterisation and stability assessment of a food derived tripeptide, Leucine-Lysine-Proline loaded chitosan nanoparticles", Minna K. Danish, Giuliana Vozza, Hugh J. Byrne, Jesus M. Frias, Sinéad M. Ryan, *Journal of Food Science: Food Engineering, Materials Science, and Nanotechnology*, June (2017) DOI: 10.1111/1750-3841.13824

This Article is brought to you for free and open access by the DIT Biophotonics and Imaging at ARROW@TU Dublin. It has been accepted for inclusion in Articles by an authorized administrator of ARROW@TU Dublin. For more information, please contact [yvonne.desmond@tudublin.ie](mailto:yvonne.desmond@tudublin.ie), [arrow.admin@tudublin.ie](mailto:arrow.admin@tudublin.ie), [brian.widdis@tudublin.ie](mailto:brian.widdis@tudublin.ie).



This work is licensed under a [Creative Commons Attribution-Noncommercial-Share Alike 3.0 License](#)



1 **Formulation, characterisation and stability assessment of a food derived**  
2 **tripeptide, Leucine-Lysine-Proline loaded chitosan nanoparticles**

3 Minna Khalid <sup>1,2</sup>, Giuliana Vozza<sup>1,2</sup>, Hugh J. Byrne<sup>2</sup>, Jesus M. Frias<sup>1</sup>, Sinéad M. Ryan<sup>3</sup>

4 <sup>1</sup> School of Food Science and Environmental Health, Dublin Institute of Technology,  
5 Marlborough Street, Dublin 1, Ireland

6 <sup>2</sup> FOCAS Research Institute, Dublin Institute of Technology, Kevin Street, Dublin 8, Ireland

7 <sup>3</sup> School of Veterinary Medicine, University College Dublin, Belfield, Dublin 4, Ireland

8

9

10 \* Corresponding author. E-mail: Jesus.Frias@dit.ie

11

12

13

14

15

16

17

18

19

20

21

22

23

24 **Abstract**

25 The chicken or fish derived tripeptide, Leucine-Lysine-Proline (LKP), inhibits the  
26 Angiotensin Converting Enzyme and may be used as an alternative treatment for pre-  
27 hypertension. However, it has low permeation across the small intestine. The formulation of  
28 LKP into a nanoparticle (NP) has the potential to address this issue. LKP-loaded NPs were  
29 produced using an ionotropic gelation technique, using chitosan (CL113). Following  
30 optimisation of unloaded NPs, a mixture amount design was constructed using variable  
31 concentration of CL113 and tripolyphosphate at a fixed LKP concentration. Resultant  
32 particle sizes ranged from 120-271 nm, zeta potential values from 29-37 mV and  
33 polydispersity values from 0.3-0.6. A ratio of 6:1 (CL113: TPP) produced the best  
34 encapsulation of approximately 65%. Accelerated studies of the loaded nanoparticles  
35 indicated stability under normal storage conditions (room temperature). Cytotoxicity  
36 assessment showed no significant loss of cell viability and *in vitro* release studies indicated  
37 an initial burst followed by a slower and sustained release.

38

39 **Keywords:** chitosan nanoparticles; food derived peptide; mixture amount design; accelerated  
40 thermal stability analysis; ACE inhibition

## 41 **1. Introduction**

42 A number of synthetic antihypertensive drugs (ACE inhibitors) are currently available on the  
43 market (e.g. captopril, lasinopril and enalapril) but all have been reported to have associated  
44 adverse side effects, such as coughing, dizziness, loss of taste and skin rashes and poor  
45 pharmacokinetics with a short half life, resulting in the requirement of frequent dosage  
46 (Bougatef et al., 2008). Therefore, natural ACE inhibitors, isolated from food sources, have  
47 attracted increasing attention in recent years, in the search to find a safer and more  
48 economical approach for the consumers (Bougatef et al., 2008). Peptides derived from food  
49 sources have been reported to have health benefits such as hypotensive activity, due to their  
50 Angiotensin Converting Enzyme (ACE) inhibitory activity (Berilyn et al., 2016; Li et al.,  
51 2016). Using DNA microarray experiments it was found that other mechanisms can also  
52 contribute to the decrease of blood pressure for bioactive tripeptides (Yamaguchi,  
53 Kawaguchi, & Yamamoto, 2009) reducing the side effects of ACE inhibition. However,  
54 exploitation of the potential nutraceutical benefits of these peptides in general is known to  
55 face a number of challenges. Insufficient gastric residence time, low permeation and/or  
56 solubility within the gut, chemical degradation within the gastrointestinal tract (GIT) due to  
57 low pH, enzymatic degradation, and the presence of other nutrients (in food), all limit the  
58 bioavailability of bioactive peptides by the oral delivery route (Braithwaite et al., 2014; Ma,  
59 2014; Segura-Campos, Chel-Guerrero, Betancur-Ancona, & Hernandez-Escalante, 2011). A  
60 number of researchers have attempted to formulate peptides into oral delivery systems for  
61 example by the addition of absorption enhancers (Choonara et al., 2014), enzyme inhibitors  
62 (Bruno, Miller, & Lim, 2013), hydrogels (Sharpe, Daily, Horava, & Peppas, 2014), liposomes  
63 (Takahashi, Uechi, Takara, Asikin, & Wada, 2009) and nanoparticles (Yao, McClements, &  
64 Xiao, 2015).

65 Leucine-Lysine-Proline is a tripeptide, derived from chicken muscle, which has shown *in*  
66 *vitro* ACE inhibitory activity, having a mean inhibitory concentration (IC<sub>50</sub>) of 0.32μM  
67 (Zhou, Du, Ji, & Feng, 2012). In addition, LKP has been shown to elicit a significant  
68 reduction of blood pressure in spontaneously hypertensive rats (SHR) when delivered  
69 intravenously, 10mg/kg<sup>-1</sup> producing a reduction in systolic blood pressure of 75mmHg,  
70 compared to an oral dose of 60mg/kg<sup>-1</sup>, which resulted in a reduction of 18mmHg (Fujita,  
71 Yokoyama, Yoshikawa, Iroyukifujita, & Eiichiyokoyama, 2000). Captopril, a synthetic oral  
72 ACE inhibitor drug used for the treatment of hypertension, has been reported by Quiñones *et*  
73 *al.* (2015) to show a maximum *in vivo* change in SHR of 60.5 ± 2.7 mmHg, 4 hours post-  
74 administration, when 50mg/kg was given orally . Recent studies have shown that LKP is  
75 stable in the GIT but with lower permeation than the market drugs, across the intestine at its  
76 target site, the small intestine (Gleeson, Heade, Ryan, & Brayden, 2015). Formulation into  
77 nanoparticles (NPs) for oral delivery can enhance the bioavailability of an encapsulated  
78 peptide drug and consequently improve its pharmacokinetics and stability (Patel, Patel, Yang,  
79 & Mitra, 2014; Ryan et al., 2013). Stable NPs with particle sizes ranging between 100-500nm  
80 (des Rieux, Fievez, Garinot, Schneider, & Pr at, 2006), zeta potential values (ZP) ≥ 30mV  
81 (Lakshmi & Kumar, 2010), polydispersity (PDI) < 0.400 (Abdel-Hafez, Hathout, &  
82 Sammour, 2014a) and maximum encapsulation efficiency are ideal characteristics for oral  
83 supplementation.

84 Chitosan is a linear polysaccharide, prepared by N-deacetylation of chitin (Rinaudo, 2006).  
85 Chitosan NPs have shown promising results for oral delivery/supplementation due their  
86 GRAS properties and their intrinsic properties, including, non-immunogenic, mucoadhesion  
87 and the ability to transiently open the tight junctions of the intestinal barrier, which can help  
88 facilitate transport of macromolecules and has the potential to act as an enhancer (Chuah,  
89 Kuroiwa, Ichikawa, Kobayashi, & Nakajima, 2009; de Moura et al., 2009; Madureira,

90 Pereira, & Pintado, 2016). LKP NPs were produced using an ionotropic gelation technique.  
91 This technique allows the preparation of chitosan NPs in aqueous solution and avoids the use  
92 of organic solvents, high dispersion energy and harsh conditions, making the technique  
93 suitable for the inclusion of nutraceuticals (García, Forbe, & Gonzalez, 2010). In this process,  
94 a chitosan with a high degree of deacetylation is used, which increases the viscosity and  
95 results in an extended conformation with a more flexible chain because of the charge  
96 repulsion in the molecule (Franca, Freitas, & Lins, 2011). Chitosan can be ionically cross-  
97 linked by counterions, such as sodium tripolyphosphate (TPP), to form a hydrogel of  
98 microparticles, and when the relative concentrations of chitosan and these anions are  
99 appropriate, NPs may be generated (Sureshkumar, Das, Mallia, & Gupta, 2010).

100 The formulation of NPs from different constituent components can be troublesome, due to the  
101 different variable parameters used (concentration, temperature and pH). Empirical  
102 optimisation using Response Surface Modelling (RSM) can help to rationalise the process  
103 and has found applications in different fields, such as engineering, pharmaceutical,  
104 biomedical, environmental and epidemiological research (Singh, Singh, Saraf, & Saraf,  
105 2011). RSM has been shown to be useful for optimisation of experimental parameters in  
106 nanoparticle formulation, and has been adopted by a number of research groups (Abdel-  
107 Hafez, Hathout, & Sammour, 2014b; Bezerra, Santelli, Oliveira, Villar, & Escalera, 2008).

108 The aim of this work is to formulate and investigate the feasibility of LKP encapsulated  
109 chitosan NPs, determining the physico-chemical characteristics, stability to storage,  
110 bioactivity and low cytotoxicity properties. The formulation of the LKP NP was optimised  
111 using a RSM approach. The physico-chemical characteristics of the NPs were assessed using  
112 dynamic laser scattering, scanning electron microscopy, and Fourier transform infrared  
113 spectroscopy, with the aim of producing the optimal NPs as an oral delivery system.  
114 Accelerated thermal conditions are employed to explore the stability for future storage

115 conditions; particle size, polydispersity, zeta potential and bioactivity were assessed. In  
116 addition, the cytotoxicity and release profiles in simulated gastric and intestinal fluids were  
117 assessed.

## 118 **2. Materials and Methods**

119 LKP (Mw 356.47, purity = 96% according to the manufacturer's specifications) was  
120 synthesised by ChinaPeptides Co. Ltd, (Shanghai, China). CL113 (Mw = 110 kDa,  
121 deacetylation degree (DD) = 86% according to manufacturer's specifications) was obtained  
122 from Pronova Biopolymer (Norway). TPP, Angiotensin-I converting enzyme (from rabbit  
123 lung), captopril, N- $\alpha$ -hippuryl-L-histidyl-L-leucine hydrate salt (HHL) and all other materials  
124 were obtained from Sigma-Aldrich (Ireland). CellTitre 96® AQu<sub>icous</sub> One Solution Cell  
125 Proliferation Assay was supplied by Promega (Madison, USA). Caco-2 cells (passage 24-26)  
126 were obtained from European Collection of Cell Cultures (Salisbury, UK). HepG2 cells  
127 (passage 32-34) were obtained from American Type Culture Collection. Ultrapure water was  
128 used for all experiments and was obtained from a Milli-Q water purification system  
129 (Millipore Corporation, USA).

### 130 2.1 Unloaded nanoparticle formulation design

131 Unloaded NPs formulation was optimised using varying concentrations of CL113 and TPP,  
132 following a 3 block Central Composite Design (CCD) with 2 variable parameters and 3  
133 responses (particle size, ZP and PDI).

### 134 2.2 LKP nanoparticle formulation design

135 A Mixture Amount Design (MAD) was employed using the concentration ranges of chitosan  
136 (CL113) and TPP (see table 1) around the optimal point (1.5mg/mL CL113 and 0.3mg/mL  
137 TPP) suggested from preliminary unloaded particle experiments (Section 3.1). The

138 experimental design and data analysis was performed using Minitab 17 software (Minitab  
139 Inc, USA).

140 **Table 1** MAD for LKP nanoparticles at optimised CL113, TPP concentration

Sample	CL113 (mg/ml)	TPP (mg/ml)	Ratio (CL113/TPP)
1	1.64	0.21	8.0
2	1.52	0.33	4.5
3	1.58	0.27	5.9
4	1.45	0.40	3.6
5	1.39	0.46	3.0

141

### 142 2.3 Preparation of LKP NPs

143 Preparation of LKP NPs was based on a modified ionotropic method (Calvo, Remu, Pez,  
144 Vila-Jato, & Alonso, 1997; Vimal et al., 2013). Stock solutions of 10mg/mL CL113 and TPP  
145 were prepared. CL113 was dispersed in acetate buffer (pH3) and TPP in 0.01M sodium  
146 hydroxide solution. The stock solutions of CL113 and TPP were diluted to different  
147 concentration ratios at a fixed volume mixture of 2.5:1 CL113: TPP containing solution. A  
148 fixed concentration of 0.1mg/mL LKP was added to the diluted TPP solutions. The  
149 TPP/peptide solution was added dropwise to the CL113 solution while stirring (800rpm for  
150 30mins). NPs were separated using ultrafiltration-centrifugation (Centriplus YM-30, MWCO  
151 of 30kDa, Millipore, USA). 10mL of sample were placed in the sample reservoir of the  
152 centrifugal filter device and centrifuged for 30mins at 3000rpm. After separation, the volume  
153 of the solution in the filtrate vial was measured and the filtrate was assayed for the amount of  
154 LKP by Reverse Phase High Performance Liquid Chromatography (RP-HPLC). The wet



155 pellet was re-suspended in purified water and immediately characterised using a range of  
156 physico-chemical techniques.

## 157 2.4 Physico-chemical characterisation of LKP NPs

### 158 2.4.1 Size, zeta potential and polydispersity index

159 The nanoparticle size (number distribution) and electrophoretic mobility measurements were  
160 performed using folded capillary cells in a Nanosizer ZS fitted with a 633 nm laser (Malvern  
161 Instruments Ltd.). Each analysis was carried out at 25°C with the equilibration time set to 2  
162 min using size by intensity distribution.

### 163 2.4.2 Fourier transform infrared spectroscopy

164 The chemical properties of the NPs were monitored using Fourier transform infrared  
165 spectroscopy (FT-IR), performed using a Perkin Elmer Spotlight 400 Series Spectrometer  
166 (with Universal Attenuated total reflectance (ATR) accessory). FT-IR spectra of LKP,  
167 unloaded NPs, and LKP NPs were obtained in the spectral range 650 to 4000  $\text{cm}^{-1}$  in  
168 triplicate. NP samples were stored at -80°C in glass vials and then lyophilised prior to  
169 analysis using a Labconco FreeZone 6 Liter Benchtop Freeze Dry System.

### 170 2.4.3 Scanning electron microscopy

171 The morphology of the freeze-dried NPs was studied using scanning electron microscopy  
172 (SEM) (Hitachi SU6600 FESEM), at an accelerating voltage of 20kV using the secondary  
173 electron detector. The freeze dried NPs (0.5mg) were dispersed in deionised water (10mL)  
174 and sonicated for 4min. One drop of the dispersion containing LKP NPs was placed on a  
175 silicon wafer and dried at room temperature. This was sputter coated with 4nm Au/Pd prior to  
176 imaging.

#### 177 2.4.4 Determination of association efficiency and loading capacity of LKP nanoparticles

178 The association efficiency (AE) and loading capacity (LC) of NPs was calculated by the  
179 indirect method of Al-Qadi *et al.* (2012). The supernatant was assayed for the content of LKP  
180 by RP-HPLC. This quantity of LKP is referred to as the non-associated peptide. The RP-  
181 HPLC analysis was performed on a Waters 1525 pump (Waters, Milford, Massachusetts)  
182 with a Photo Diode Array detector 2487 (Waters) using a Luna C18 column (5 $\mu$ m, 250mm x  
183 4.6mm, Phenomenex). Analytes were detected at the wavelength of  $\lambda_{\text{max}}= 220\text{nm}$ . The  
184 column was eluted at a flow rate of  $1\text{mL}\cdot\text{min}^{-1}$  with an isocratic system (15% Acetonitrile,  
185 0.05% TFA in water). The AE% and loading capacity (LC %) was calculated using the  
186 following equations.

$$187 \text{ AE \%} = \frac{(\text{Total amount Peptide} - \text{free amount Peptide in supernatant})}{\text{Total amount of Peptide}} \times 100 \quad (4.1)$$

$$188 \text{ LC\%} = \frac{(\text{Total amount Peptide} - \text{free amount Peptide in supernatant})}{\text{Nanoparticle weight}} \times 100 \quad (4.2)$$

#### 189 2.4.5 ACE inhibition assay

190 The ACE inhibition of LKP was determined as previously described with minor  
191 modifications (Henda *et al.*, 2013; Lahogue, Réhel, Taupin, Haras, & Allaupe, 2010). All  
192 solutions were pre-filtered with 0.22 $\mu$ m nylon syringes prior to analysis. HHL (5mM) was  
193 dissolved in pH 8.3 buffer (0.1M borate buffer in 0.3M NaCL). In a 96-well plate, 100 $\mu$ l  
194 substrate solution and 25 $\mu$ l inhibitor were incubated for 10min at 37°C. 10 $\mu$ l ACE solution  
195 (100mU/mL) was then added and incubated for another 30min at 37°C. The assay was  
196 terminated using 100 $\mu$ l of 1M HCL. HPLC was performed using a C8 column (2.7 $\mu$ m, 3.0 x  
197 100mm, Agilent Technologies UK & Ireland Ltd) and wavelength detection at  $\lambda_{\text{max}}= 228\text{nm}$ .  
198 An isocratic method was used at a flow rate of  $0.4\text{mL}\cdot\text{min}^{-1}$ , 25% Acetonitrile, 0.1% TFA in  
199 water for 5min. Controls were prepared by replacing the inhibitor with assay buffer (negative

200 control) and captopril (positive control). 100% ACE inhibition (negative control) was used to  
201 calculate the % of ACE activity.

$$202 \text{ ACE inhibition (\%)} = \left(1 - \frac{A_{\text{inhibitor}}}{A_{\text{blank}}}\right) * 100 \quad (4.3)$$

203 where  $A_{\text{inhibitor}}$  and  $A_{\text{blank}}$  are the peak areas of HA (product of HHL) and negative control,  
204 respectively. The  $IC_{50}$  of the inhibitor was determined using the Hill-Step equation (Prism 5,  
205 GrapPad Software Inc., USA).

#### 206 2.4.6 Accelerated stability analysis

207 The optimal formulation was further analysed under accelerated stability conditions. 10mL of  
208 a NP formulation equivalent to 19.5mg of NPs were resuspended in aqueous solution (pH7)  
209 and stored at accelerated conditions; 60°C for 720min, 70°C for 300min and 80°C for  
210 120min. The particle size and colloidal stability over different time intervals were measured  
211 using the Nanosizer ZS (Malvern Instruments Ltd), and the order of degradation in aqueous  
212 LKP suspension was determined. The end point of each sample was further assessed for ACE  
213 inhibition activity (Method 2.4.5). Stability analysis was analysed using R software (R Core  
214 Team, 2015).

215 The kinetic model used to describe the stability was of zero order. The temperature  
216 dependence of the kinetic parameters of LKP NPs stability was measured by calculating the  
217 observed rate constants. This was plotted according to the Arrhenius equation and apparent  
218 activation energy,  $E_a$  and reaction rate,  $k_{\text{ref}}$  were calculated according to Equation 4 (Brauner  
219 & Shacham, 1997).

$$220 C = C_0 + e^{\ln(k) - \frac{E_a}{R} \left( \frac{1}{T} - \frac{1}{T_{\text{ref}}} \right)} t \quad (4.4)$$

221 where C is the property (particle size or PDI) at time t,  $C_0$  is the initial property conditions, k  
222 is the apparent zero order reaction constant,  $E_a$  is the energy of activation, R is the universal

223 gas constant, T is the temperature of the experiment (K) and  $T_{ref}$  is the reference temperature  
224 (70°C).

#### 225 2.4.7 MTS assay

226 Caco-2, heterogeneous human epithelial colorectal adenocarcinoma cells and HepG2, a  
227 human liver cancer cell line, were seeded at a cell density of  $2 \times 10^4$  cells/well and cultured  
228 on 96 well plates in DMEM and EMEM respectively, supplemented with 10% fetal bovine  
229 serum, 1% L-glutamine, 1% penicillin-streptomycin and 1% non-essential amino acids, and  
230 incubated for 24h at 37°C in a humidified incubator with 5% CO<sub>2</sub> and 95% O<sub>2</sub>. Specified  
231 exposure times were used for Caco-2 and HepG2, in order to mimic *in vivo* conditions. The  
232 maximum time NPs will be exposed to the intestines are 4h, hence a 4h exposure time was  
233 used in Caco-2 cell lines (Neves, Martins, Segundo, & Reis, 2016). In addition to this, 72h  
234 exposure time was used for HepG2 cell line to mimic the liver (Brayden, Gleeson, & Walsh,  
235 2014). LKP (native), unloaded NP and LKP NPs at 1, 5 and 10mM concentration were  
236 assessed. Triton X-100™ (0.05%) was used as a positive control. After exposure, treatments  
237 were removed and replaced with MTS (3-(4,5-dimethylthiazol-2-yl)-5-(3-carbo  
238 xymethoxyphenyl)-2-(4-sulfophenyl)-2H-tetrazolium. Optical density (OD) was measured at  
239 490 nm. Each value presented was normalised against untreated control and calculated from  
240 three separate experiments, each of which included six replicates.

#### 241 2.4.8 *In vitro* controlled release studies

242 LKP release from loaded formulation was carried out using a dialysis bag diffusion technique  
243 (Hosseinzadeh, Atyabi, Dinarvand, & Ostad, 2012) over 24h (Calderon *et al.*, 2013; Yoon *et*  
244 *al.*, 2014). To ensure sink conditions, NPs were solubilised and sonicated 3 times for 20  
245 seconds (Branson Ultrasonics; Ultrasonic processor VCX-750W, Wilmington, North  
246 Carolina, USA). 5mL of LKP formulation was placed in the dialysis bag (cellulose ester

247 membrane, molecular weight cut-off 100kDa, Float-A-Lyzer<sup>®</sup>G2, Sigma-Aldrich, Ireland)  
248 and immersed in a vessel containing 50mL of release fluid using simulated gastric fluid  
249 (SGF) or simulated intestinal fluid (SIF) specified according to the British Pharmacopoeia,  
250 respectively. SGF was composed of 0.1 M HCL and SIF, as the buffering stage, was  
251 composed of 1 volume of 0.2 M trisodium phosphate dodecahydrate and 3 volumes of 0.1 M  
252 HCL (adjusted to pH 6.8), without enzymes (British Pharmacopoeia Commission, 2016).  
253 Each experiment was agitated at 100rpm, 37°C using a thermostatic shaker. At predetermined  
254 time points over 24h, 1mL of release fluid was analysed and replaced with simulated fluid.  
255 The LKP release was measured using RP-HPLC. The following equation was employed to  
256 determine the % cumulative drug release:

$$257 \quad \% \text{ cumulative release} = \frac{\text{LKP release}}{\text{LKP initial}} * 100 \quad (4.5)$$

258 where LKP release and initial represents the concentration of LKP release and the amount of  
259 LKP initially loaded into the NPs, respectively.

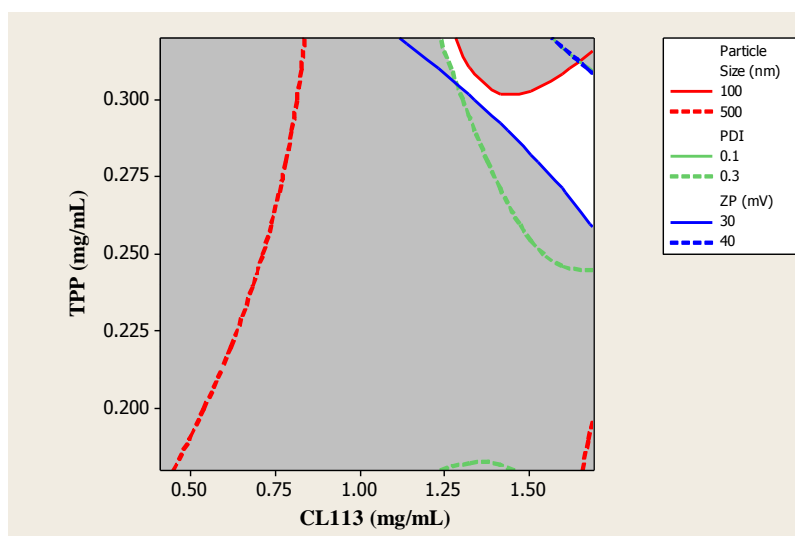
### 260 **3. Results and discussion**

261 LKP has an isoelectric point (pI) of 9.17, calculated using the Henderson-Hasselbach  
262 equation (Henriksson, Englund, Johansson, & Lundahl, 1995). This is the net charge of a  
263 molecule indicating that, at a pH of 9.17, LKP will have minimal solubility. At pH values  
264 below the pI, peptides carry a net positive charge and above the pI, a negative charge. LKP  
265 has a similar charge to TPP, and hence LKP was dissolved in the TPP solution. TPP-LKP  
266 was then added dropwise to the CL113 solution, resulting in the formation of opalescent NPs.

#### 267 **3.1 Unloaded nanoparticle production feasibility zone identification**

268 The formulation of CL113 NPs was optimized using a CCD factorial design to analyse the  
269 effect of the pH, CL113: TPP ratio and acetic acid concentration on the size and ZP of the  
270 particles. Preliminary studies were conducted to select the most feasible region for the

271 formulation of peptide NPs (figure 1). This showed that > 1.25 mg/mL CLL113 and 0.25-0.3  
272 mg/mL TPP resulted in unloaded NPs of optimal sizes of 300 nm and ZP > 30 mV.

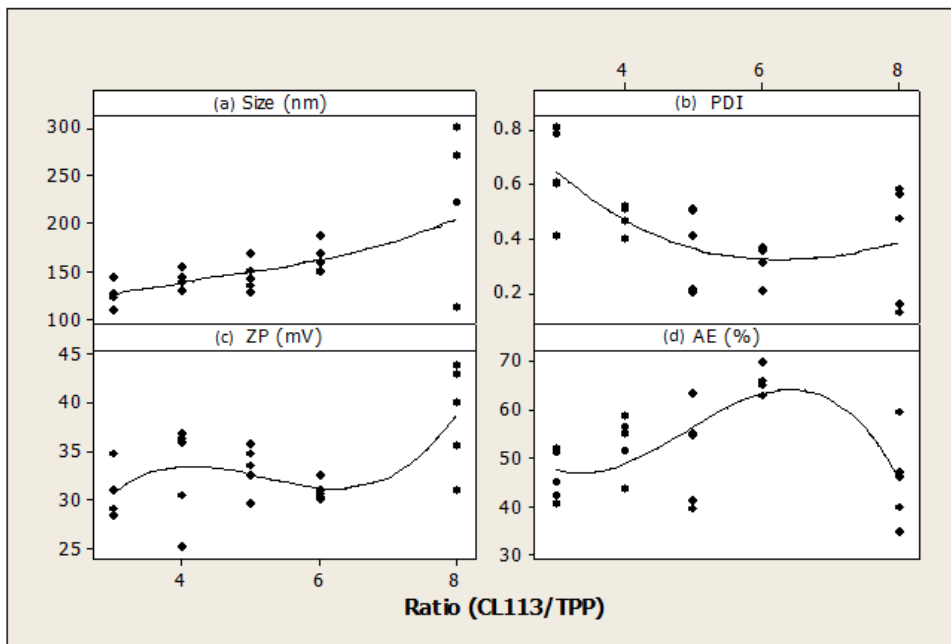


273  
274 **Figure 1** Overlaid contour plots of Size and ZP: the targeted area is highlighted (white).

275 This result is in agreement with Calvo et al., (1997) who reported that concentrations which  
276 exceed 4mg/mL and 0.75mg/mL respectively for chitosan and TPP resulted in the formation  
277 of large aggregates. Nanoparticles of the desired characteristics were found to be produced at  
278 concentrations of 0.28 mg/mL (TPP) and 1.25 mg/mL (Chitosan). In addition, studies done  
279 by de Pinho Neves et al. (2014) showed similar results within the 5 to 6:1 ratio. Unloaded  
280 CL113 NPs were used as control for peptide-loaded experiments.

### 281 3.2 Nanoparticle size, zeta potential analysis and AE % of LKP nanoparticles

282 From the preliminary optimisation analysis of unloaded CL113 NPs; a CL113 concentration  
283 of 1.5mg/mL was chosen as the centre point for the MAD. LKP NP size values ranged from  
284 120 to 271nm, with ZP values above 30mV. With regards to the AE % (figure 2), at ratios  
285 above 5.9, there is less variability (error bars), but at a ratio of 8, stable agglomerates (>  
286 30mV ZP) of variable sizes are observed.



287

288 **Figure 2** Scatterplot of (a) Size (nm), (b) PDI, (c) ZP (mV) and (d) association efficiency  
 289 (AE %) of LKP NPs against different ratios of (CL113/ TPP). Error bars represent the  
 290 individual 95% Confidence interval for the average

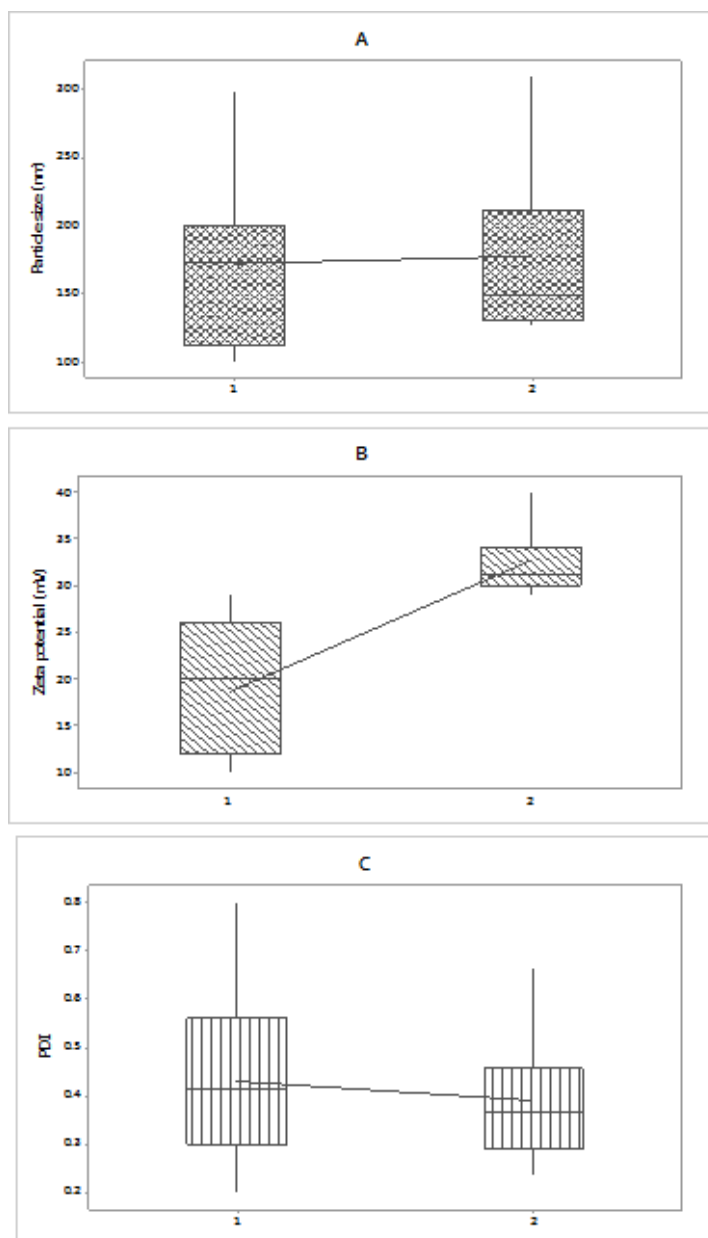
291 An initial observation of the results at different ratios seems to indicate that the ratio of 5.9 is  
 292 the best performing in terms of higher AE% and lower PDI, while still maintaining a particle  
 293 size (150nm) and a ZP (>30mv) that indicates stability (figure 2). LC% for all experiments  
 294 showed no significant differences, values ranged from 2-3% (see supplementary material, S2)  
 295 were attained. Studies from other groups showed that an increase of counterion (TPP)  
 296 concentration results in a decrease of LC due to the high level of crosslinking, causing the  
 297 encapsulated material to come out of the particle (Woranuch & Yoksan, 2013).

298 Similar profiles are seen for the 3 responses, size (nm), ZP (mV) and PDI, suggesting  
 299 agglomeration and colloidal instability above a ratio (CL113/TPP) of 7. The degree of  
 300 crosslinking can be assessed by the chitosan concentration and the available NH<sub>3</sub><sup>+</sup> able to be  
 301 crosslinked with TPP functional groups. At intermediate operation conditions, i.e. ratios  
 302 between 7 and 5.5, most responses present a lower variation between replicates with respect

303 to all responses and a minimum PDI. Analysis for all experimental results shows particle  
304 sizes within the optimal size range (100-500nm) and ZP above 30mV values. However, for  
305 some experimental conditions, the AE% and PDI exhibited values far from the optimal  
306 physico-chemical characteristics and had high variability between replicates (N=3). At  
307 (CLL113/TPP) ratios above 7 and below 4.5, the NPs exhibited higher PDI and, below a ratio  
308 of 6, significant variability of AE% amongst replicates is evident.

309 The results obtained were consistent with those observed for unloaded CL113 NPs in terms  
310 of particle size, although a significant increase in colloidal stability for the loaded NPs was  
311 observed (see figure 3).





312

313 **Figure 3** Boxplot for LKP NPs where each Group represents 1: control (unloaded NPs) and

314 2: LKP NPs. The changes of each group are examined for A: particle size, B: ZP and C: PDI.

315 A significant increase in ZP is seen for loaded NPs with a decrease of variability.

316 For the MAD design, a third order polynomial regression model was employed to describe

317 the variation of size (nm), ZP (mV), PDI and AE % of the LKP NPs against the ratio

318 (CL113/TPP). The polynomial equation parameters for each response against ratio were

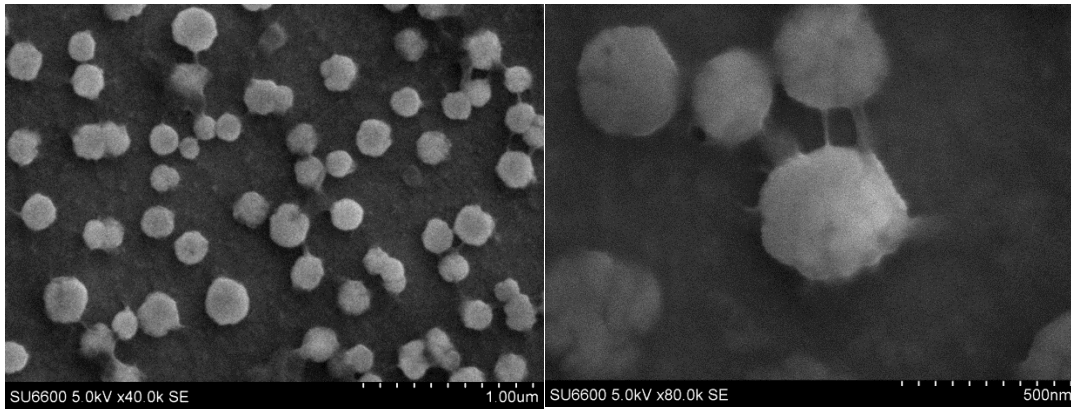
319 fitted. The models were built with the aim of identifying conditions within the experimental

320 design where NPs would be present as monodispersed, stable NPs with maximum peptide  
321 encapsulation (see supplementary information S1).

322 From the results obtained, a ratio of 5.9 provided the most promising results, for optimal oral  
323 delivery fulfilling the formulation constraints; 100-500 nm, PDI <0.4 and |ZP| >30 mV. In  
324 comparison, NPs produced at a ratio of 7.8, presented the highest variability for size ( $206 \pm$   
325  $73$  nm), PDI ( $0.4 \pm 0.2$ ), ZP ( $38 \pm 6$  mV) and AE ( $41 \pm 11\%$ ). Notably, the NPs produced at a  
326 ratio of 5.9 (CL113/TPP) yielded a substantially higher AE % of around 65%. It should be  
327 noted that the LKP of isoelectric pH (9.17) was added to a higher pH TPP (pH 12) solution.  
328 This provided more negatively charged molecules to interact with chitosan, consequently  
329 increasing the AE % (Acton, 2012). This finding is in agreement with Silva et al.,(2013), who  
330 observed higher AE % of daptomycin at higher pH values relative to the isoelectric pH. In  
331 addition, LKP has a low Mw and studies of lower Mw actives showed higher AE %. This  
332 trend was observed by Jarudilokkul et al., (2011), who showed that  $\alpha$ -Lactalbumin (17.4 kDa)  
333 has higher AE % than Fibrinogen (340 kDa).

### 334 3.3 Morphological characterisation of LKP chitosan nanoparticles

335 Further characterisation of the NPs produced with the optimal (CL113/TPP) ratio of 5.9 was  
336 performed. Figure 4 represents an SEM image of LKP formulation, confirming the formation  
337 of the NPs. Spheroidal NPs were obtained, of sizes ranging from 150-250nm, consistent with  
338 the DLS measurement.



339

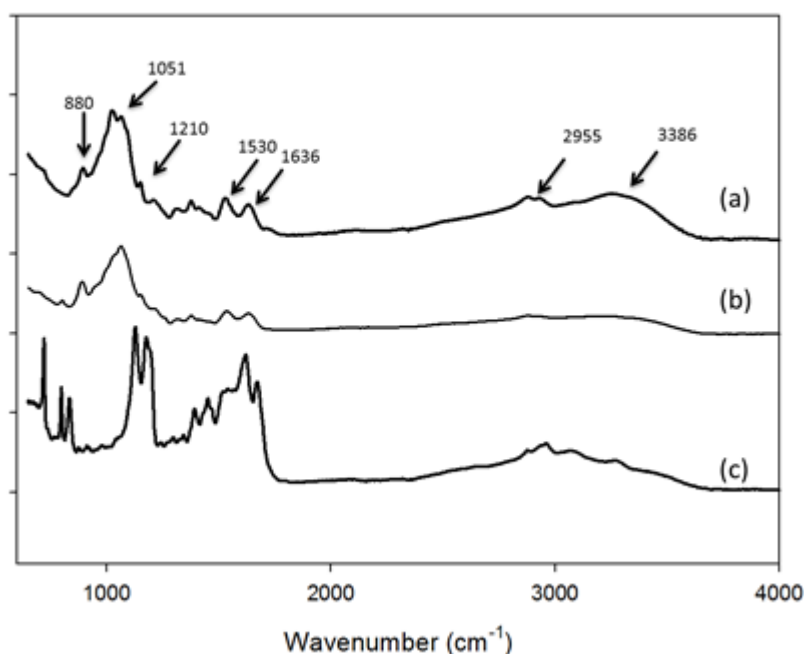
340 **Figure 4** SEM image of optimal formulation (Ratio 5.9) of LKP NPs

### 341 3.4 Chemical Characterisation of LKP nanoparticles

342 FT-IR was used to identify whether there were variations in chemical functional groups  
343 presented in the LKP loaded NPs with respect to their raw materials. An FT-IR analysis was  
344 conducted for pure LKP powder, unloaded NPs and LKP NPs (Figure 5). Chitosan NPs have  
345 been previously characterised using FT-IR (Mohammadpour Dounighi et al., 2012;  
346 Sureshkumar et al., 2010; Vimal et al., 2013).

347 Comparison of the FT-IR spectra of loaded and unloaded NPs indicated that the spectrum of  
348 the unloaded NPs is largely unchanged by the presence of LKP, as may be expected due to  
349 the relatively low LKP content. Characteristic peaks of unloaded NPs are seen in both, at  
350  $1530$ ,  $1636$  and  $880\text{cm}^{-1}$ , representing the amide I and amide II bands of CL113 and pyranose  
351 (P-O) of TPP. For the optimal formulation,  $18.5\text{mg}$  of NPs is needed to encapsulate  $1\text{mg}$  of  
352 LKP. Hence, no distinctive peaks of LKP can be seen in the LKP spectrum. The FT-IR  
353 spectrum of LKP NPs does, however, show some changes from that of the unloaded NPs,  
354 potentially indicative of localised conformational changes of the CL113 as a result of  
355 interaction with the LKP (figure 5). An increased absorption at  $3386\text{cm}^{-1}$  compared to that of  
356 the unloaded NPs is observed. Absorption in this region of the spectrum represents O-H  
357 bonding; a possible explanation may be due to the interaction of the hydrogen acceptors (O-

358 in LKP) and hydrogen donors ( $\text{NH}_3^+$  in chitosan). In addition, increased absorption is also  
359 seen for LKP NPs at  $2955\text{cm}^{-1}$ , representing an increase in (C-H) hydrogen bond stretching  
360 with presence of the peptide. A shift of  $1605\text{cm}^{-1}$  to  $1530\text{cm}^{-1}$  was also observed which  
361 represent the amide carbonyl stretch (Mohammadpour Dounighi et al., 2012). The peaks at  
362  $1210\text{cm}^{-1}$  and  $880\text{cm}^{-1}$  represent phosphate group (P-O) and pyranose ring (Woranuch &  
363 Yoksan, 2013). The peak at  $1051\text{cm}^{-1}$  shows a split for the loaded NPs, suggesting a  
364 conformational change due to the interaction with the LKP.



365  
366 **Figure 5** FT-IR spectra of (a) LKP NPs (b) unloaded NPs and (c) Pure LKP powder.  
367 Absorbance spectra are normalised and offset for clarity.

### 368 3.5 $\text{IC}_{50}$ determination of inhibitor

369 The inhibitory activities of captopril (reference molecule) and LKP were determined using a  
370 synthetic substrate, HHL, and varying concentrations over the range  $0.0001 - 10\mu\text{M}$   
371 (captopril) and  $0.001 - 10\mu\text{M}$  (LKP). The  $\text{IC}_{50}$  obtained was  $0.006 \pm 0.002 \mu\text{M}$  for captopril  
372 and  $0.30 \pm 0.08 \mu\text{M}$  for LKP. These values are consistent with previously reported values,

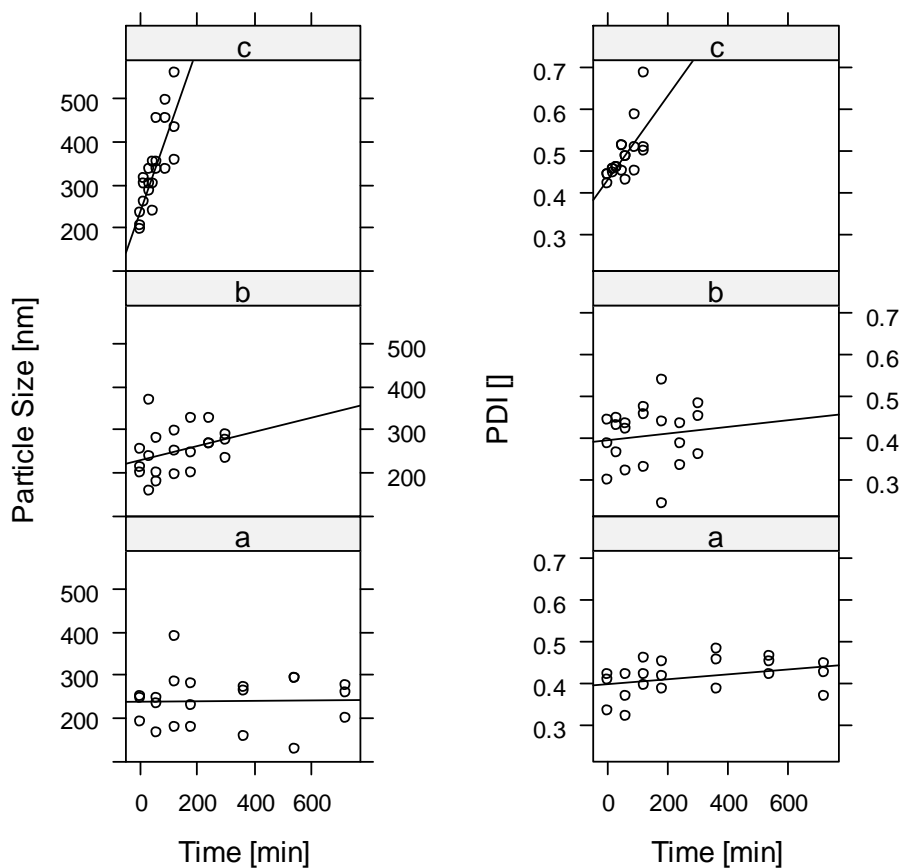
373 which range from 0.001-0.039 $\mu$ M for Captopril and 0.2-0.32 $\mu$ M for LKP (Fujita &  
374 Yoshikawa 1999; Fujita *et al.* 2000; Henda *et al.* 2013).

### 375 3.6 Accelerated stability analysis of LKP NPs

376 In accelerated stability testing, a product is stressed at high temperatures and  
377 degradation/stability of the product at normal storage conditions is then predicted (Bajaj,  
378 Singla, & Sakhuja, 2012; Rauk, Guo, Hu, Cahya, & Weiss, 2014; Waterman & Adami,  
379 2005). A number of factors can affect the solution stability of NPs, for example, the pH of the  
380 aqueous solvents, light, oxygen, co-solutes, buffer salts, surfactants and antioxidants.  
381 Common degradation routes include hydrolysis/solvolysis, photolysis/oxidation and  
382 racemisation (Weber, Coester, Kreuter, & Langer, 2000). A number of groups have found  
383 that CL113 NPs synthesised by ionic gelation lose their integrity in aqueous media, even in  
384 the absence of enzymes (López-León, Carvalho, Seijo, Ortega-Vinuesa, & Bastos-González,  
385 2005). Jonassen *et al.* (2012) looked at the effect of different ionic strength over the course of  
386 a month; the main findings were that the most stable NPs with respect to the size and  
387 compactness of the particles were produced in saline conditions (Jonassen, Kjøniksen, &  
388 Hiorth, 2012). A similar study was also conducted, preparing NPs in different ionic strength  
389 and buffers, and results showed that the least stable NPs were produced in non-buffered  
390 solutions or low ionic solutions (López-León *et al.*, 2005).

391 The stability of formulations can be tested using a number of testing protocols, which include  
392 real time stability testing, accelerated stability testing, retained sample stability testing and  
393 cyclic temperature stress testing (Bajaj *et al.*, 2012). In the current study, accelerated stability  
394 testing was used, by which NPs are subjected to stress and then assayed simultaneously to  
395 predict the likelihood of instability based upon the Arrhenius equation. Suspensions of NPs in  
396 buffered solutions (PBS pH 7), formulated at a ratio of 5.9 CL113:TPP (optimal LKP loaded

397 NPs), were exposed to three different storage temperatures, 60°C, 70°C and 80°C, over a  
398 time course of 120, 300 and 720min at each temperature. Figure 6 shows the kinetic  
399 behaviour of the particle sizes at different temperatures. The stability of the NPs decreased  
400 with increasing temperature. At 60°C, no change in particle size was observed over the  
401 720min. Figure 6 indicates a more pronounced increase in both particle size and PDI at 70°C,  
402 while at 80°C, both particle size and PDI increase significantly over the time course. At this  
403 temperature, the particle size was seen to increase monotonically from 200 to 600nm, while  
404 the PDI increases from 0.4 to 0.7. While some curvature is apparent in the trends at the  
405 highest temperature, within the present experimental error, an apparent zero order mechanism  
406 fitted better to all the data, compared to an apparent first or second order model.



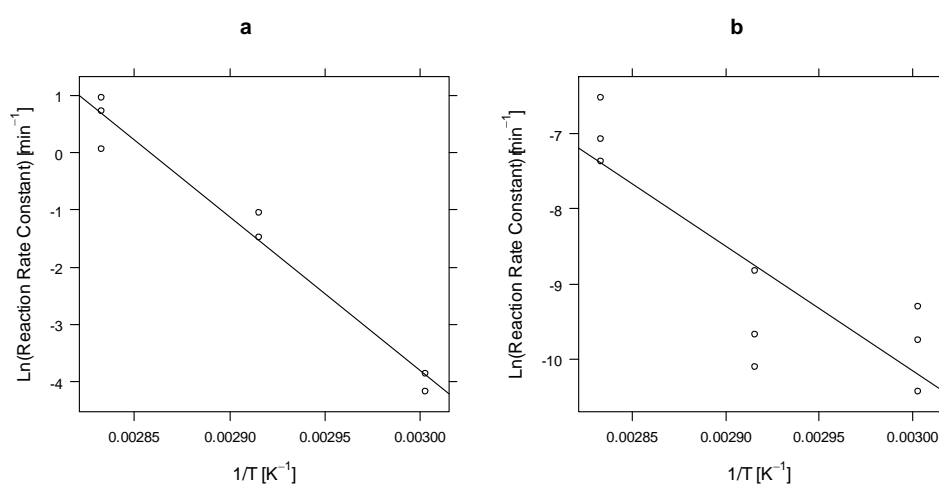
407

408 **Figure 6** Particle size and PDI analysis of LKP loaded NPs exposed at (a) 60°C (b) 70°C and  
 409 (c) 80°C over time periods of 120, 300 and 720min, respectively. N= 3

410 An Arrhenius plot of the apparent zero order reaction rate constants, derived from the  
 411 analysis of the individual experiments at the different temperatures, indicates that the kinetics  
 412 of the particle size and PDI followed this temperature relationship, consistent with an energy  
 413 activated process, with similar energies of activation for particle size and PDI (see Figure 7).

414 The one-step nonlinear regression analysis of the kinetic experiments shows that the particle  
 415 size fits to a zero order kinetic behaviour and an Arrhenius dependence with  $\ln(k_{\text{ref}@70\text{C}}) = -$   
 416  $3 \pm 1 \text{ min}^{-1}$  and an  $E_a$  of  $= 360 \pm 103 \text{ kJ/mol}$ . For the PDI, a one-step nonlinear regression was  
 417 fitted to zero order kinetics with an Arrhenius dependence of  $\ln(k_{\text{ref}@70\text{C}}) = -8.9 \pm 0.3 \text{ mins}^{-1}$   
 418  $^1$  and  $E_a = 196 \pm 33 \text{ kJ/mol}$ . A linear correlation is evident between  $1/T$  and  $\ln k$  in figure 7.

419 From this analysis, it suggests the nanoparticle formulation would be stable (in terms of  
420 particle physico-chemical properties) in a neutral pH solution at ambient storage temperature,  
421 with negligible increases in particle size or PDI of the NPs, confirming the higher stability of  
422 NPs prepared in buffered solutions. Only after 90min destabilisation of NPs was observed at  
423 the highest temperature conditions. These results are in agreement with previous literature,  
424 reporting that when NPs are produced in salt or buffered environment, stability is improved  
425 (López-León et al., 2005).

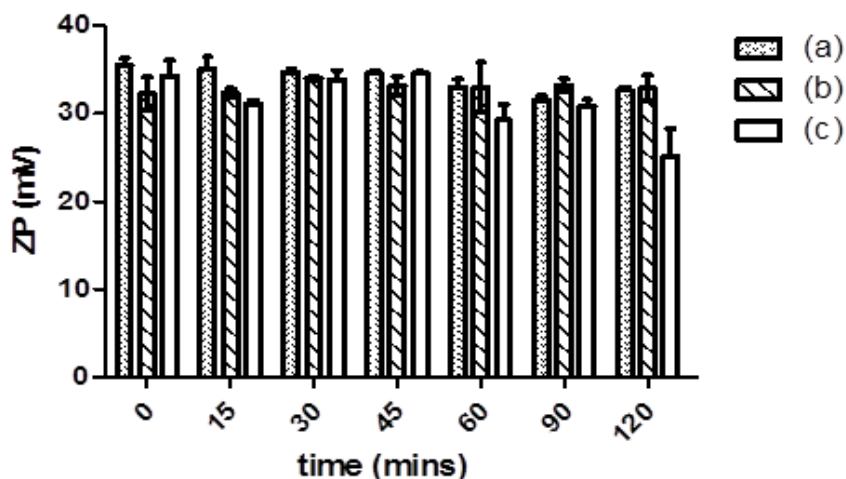


426

427 **Figure 7** Arrhenius Plots for the (a) Particle Size and (b) PDI accelerated studies of LKP  
428 loaded NPs. N=3

429 The results suggest either (i) swelling of the chitosan NPs in the aqueous environment (Bajpai  
430 & Maan, 2012) or (ii) agglomeration of chitosan NPs due to electrostatic interactions with an  
431 increase of temperature. In order to confirm the type of degradation, the zeta potential was  
432 assessed. Destabilisation of NP suspensions which would give rise to aggregation should be  
433 reflected in changes in ZP values when NPs aggregate. However, no significant changes were  
434 seen for the colloidal stability (i.e. ZP of LKP NPs). This suggests that swelling could be the  
435 primary mechanism of the CL113 nanoparticle changes with time, followed by destabilisation  
436 at higher temperatures and longer time (see figure 8).





437

438 **Figure 8** Zeta potential analyses of LKP-loaded NPs at (a) 60°C, (b) 70°C and (c) 80°C. No  
 439 significant changes were observed with One-Way ANOVA with Dunnetts's post-test. Each  
 440 value represents the mean  $\pm$  SD (n=3)

441 In addition, DD of CL113 used for this experiment is greater than 85%, it has been  
 442 previously reported that with an increase of DD the aggregation stability decreases due to the  
 443 CL113 more prone to TPP bridging which causes it to become more lyophobic near  
 444 physiological pH which may contribute to the stability of the NPs (Haung, Cai, & Lapitsky,  
 445 2015). Overall, the accelerated experiments on LKP NPs indicate that the formulations will  
 446 be stable under normal storage conditions. This could be due to the conditions (presence of  
 447 salt) used to prepare the NPs, in addition to the strong bonding between the bioactive and  
 448 complex.

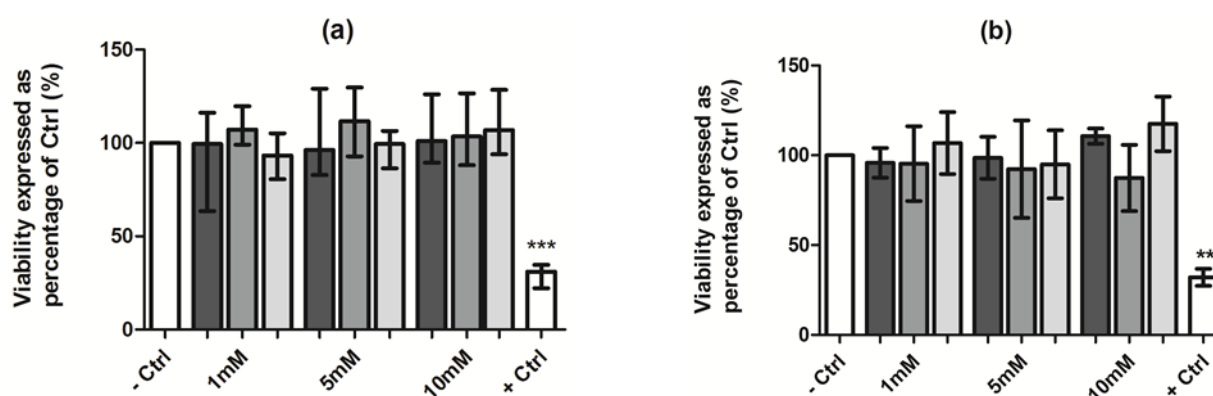
### 449 3.7 Cytotoxicity assessment of LKP nanoparticles

450 The MTS assay was used to assess the cytotoxicity of LKP and LKP NPs. The therapeutic  
 451 dose of LKP is 10mg/kg (Fujita et al., 2000; Fujita & Yoshikawa, 1999b). Hence, LKP  
 452 loaded or unloaded NPs at the different concentrations (1, 5 and 10mM) when exposed to  
 453 Caco2 (4h) and HepG2 (72h) cell lines. No cytotoxicity was observed for LKP, indicating

454 negligible overall cytotoxicity of the formulation (figure 9). No significant changes were  
 455 observed. A number of deviations were observed above 100% viability for NPs with and  
 456 without LKP, proliferation may occur due to increase in fibroblasts production caused by the  
 457 presence of polymeric chitosan (Rajam, Pulavendran, Rose, & Mandal, 2011) or interference  
 458 of NPs with the cell assay (Casey et al., 2007).

459

460



461

462 **Figure 9** Cytotoxicity assessment of  LKP,  unloaded NPs and  LKP NPs  
 463 exposed for (a) 4h in Caco2 cell lines and (b) 72h in HepG2 cell line at 1mM, 5mM and  
 464 10mM concentration. Percentage (%) of MTS converted was compared to untreated control.

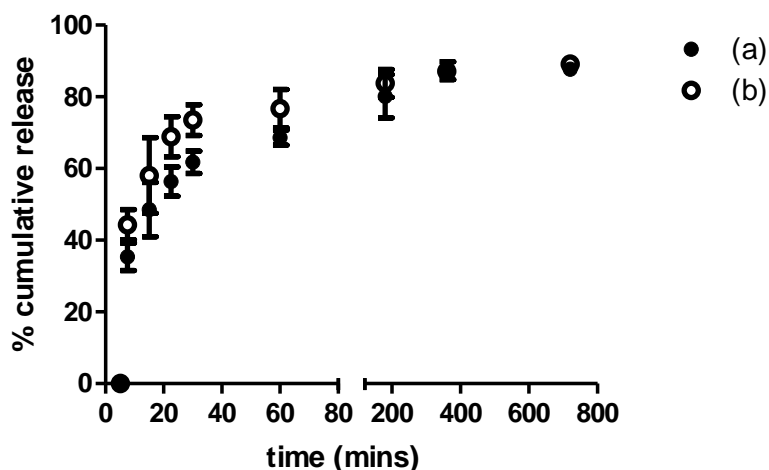
465 1-Way ANOVA with Dunnetts's post-test \*\*\* P< 0.001, \*\* P< 0.01, N=3

### 466 3.8 *In vitro* release studies

467 The release of a bioactive can take place by several different mechanisms, for example  
 468 surface erosion, disintegration, diffusion and desorption (Hosseini, Zandi, Rezaei, &  
 469 Farahmandghavi, 2013). Such a phenomenon can be influenced by a number of factors such  
 470 as the type of polymer used, the polymeric swelling capability, the solute diffusion and  
 471 material degradation (Fu & Kao, 2009; Siepmann & Göpferich, 2001). The *in vitro* LKP  
 472 release profiles of the NP formulation in SGF and SIF were measured over 24h, using RP-  
 473 HPLC at 220nm at different time points. The site of target for LKP is in the jejunum, small

474 intestine, therefore it is important to bypass the acidic stomach environment. LKP NPs results  
475 showed an initial burst followed by a slow release. Similar results were reported by other  
476 groups, Hosseini *et al.* 2013 and Luo *et al.* 2010. Hosseini *et al.* 2013, they observed a  
477 “biphasic release” mechanism (initial burst followed by slower release) with oregano  
478 essential oil when encapsulated into CL113 NPs. Luo *et al.* 2010, encapsulated selenite in  
479 chitosan NPs, demonstrating the effect of CL113 concentration on the release profile. They  
480 found that, at high concentrations of chitosan, more dense particles were found which  
481 ultimately lowered the epithelial membrane permeability. Conflicting results have been  
482 reported of the release mechanism of chitosan nanoparticles. Some groups observed the  
483 inability of chitosan based nanoparticles to sustain the release of an active following an initial  
484 burst release at higher ratios of CL113 and TPP (Stoica & Ion, 2013). Others reported a  
485 controlled release; for example, Nallamuthu, Devi, & Khanum, (2015) observed the 69%  
486 release of chlorogenic acid over 100 h. Release profiles at 1.5mg/ml CL113 also showed a  
487 burst within the first 30min in the SGF followed by a slower release from 30min to 2h then a  
488 more slow sustained release up to 24h, as shown in figure 10. For LKP NPs, the initial burst  
489 may possibly represent loosely bound LKP around the CL113 NP. Within the first hour, 62%  
490  $\pm 3$  and 74%  $\pm 4$  LKP was released in (a) SGF and (b) SIF, significance was observed for SGF  
491 vs SIF using a t-test, where  $P = 0.0074$ , respectively (figure 10). 12% more release was  
492 observed in the SIF (site of target) at pH 6.8. Chitosan has an isoelectric point of 6.5, at  
493 which pH chitosan holds a charge of zero (no charge), causing it to become unstable and  
494 precipitate out; consequently releasing more of the loaded peptide. It has been suggested by  
495 Gan & Wang, (2007) that a burst release of protein molecules may correspond to the fast  
496 swelling and degradation of the nanoparticles. This swelling phenomenon can be observed in  
497 (figure 10) After 1h, a slower release is observed, this may be attributed to the more strongly  
498 bound LKP loaded within the CL113 nanoparticle. A burst release has previously been

499 reported from other groups working with chitosan NPs, Sarmiento *et al.* (2007) showed a  
500 similar undesirable burst of 50% insulin chitosan NPs when complexed with alginate. Ryan *et*  
501 *al.* (2013) also reported an initial burst of 40% of salmon calcitonin when complexed into a  
502 NPs system using chitosan and hyaluronic acid. For oral delivery systems, NPs remain in the  
503 system for up to 6h after intake. Our studies show after 6h up to 85% release was obtained.  
504 However, a prolonged release is desired. Additional of an outer surface coating is a technique  
505 which has been widely used by a number of researchers in order to improve the integrity of  
506 the NPs and to better control the release profile (Elgadir *et al.*, 2015). A popular approach to  
507 yield coated chitosan NPs is by polyelectrolyte complexation, which exploits the interaction  
508 between positively charged chitosan and negatively charged polyelectrolytes such as alginate  
509 (Garrait, Beyssac and Subirade, 2014), dextran (Sarmiento *et al.*, 2006), hyaluronic acid  
510 (Mero *et al.*, 2014) or zein (Luo, Teng and Wang, 2012). Further work on LKP encapsulation  
511 will involve the polyelectrolyte complexation of LKP to achieve the desired release.  
512 .



513

514 **Figure 10** Cumulative release profile of LKP from NPs in (a) SGF and (b) SIF for 24h.

#### 515 **4. Conclusions**

516 LKP loaded NPs were formulated successfully by applying the ionotropic gelation technique.  
517 The optimal NPs were found at a ratio 5.9:1 (CL113: TPP), using the design of experiment  
518 approach, which resulted in reproducibility of the desirable physico-chemical characteristics.  
519 Optimally LKP NPs were spheroidal particles of size ~200nm, as shown by SEM, and had  
520 enhanced colloidal stability compared to the unloaded particles. A 5.9:1 ratio provided high  
521 encapsulation efficiency of  $65\pm 3\%$  with loading capacity of approximately  $5\pm 0.8\%$ . Stability  
522 analysis showed long term physico-chemical stability. ACE inhibitory studies presented no  
523 change in bioactivity of LKP over the different temperature conditions and after formulation  
524 indicating it is quite stable. In addition, no cytotoxicity was observed from both the LKP  
525 loaded and unloaded NPs. *In vitro* release studies indicated an initial burst within 1h,  
526 suggesting the presence of more loosely bound tripeptide in the nanoparticle complex,  
527 followed by peptide bounded within the nanoparticle which is released at a slower rate.  
528 Chitosan based delivery systems is a feasible for the formulation of bioactive peptide,  
529 physicochemical analysis and stability was efficient. The present results indicate that the  
530 addition of an enteric coating to is recommended in order to bypass the stomach acidic pH  
531 conditions, providing an efficient delivery system.

#### 532 **Acknowledgements**

533 This project is funded by an Irish Department of Agriculture Food Institutional Research  
534 Measure (FIRM) grant 'NUTRADEL' grant number 11F042. Special thanks to Dr Anne  
535 Shanahan for the assistance in image analysis.

#### 536 **References**

537 Abdel-Hafez, S. M., Hathout, R. M., & Sammour, O. a. (2014a). Towards better modeling of  
538 chitosan nanoparticles production: Screening different factors and comparing two

539 experimental designs. *International Journal of Biological Macromolecules*, 64, 334–  
540 340. <http://doi.org/10.1016/j.ijbiomac.2013.11.041>

541 Abdel-Hafez, S. M., Hathout, R. M., & Sammour, O. a. (2014b). Towards better modeling of  
542 chitosan nanoparticles production: Screening different factors and comparing two  
543 experimental designs. *International Journal of Biological Macromolecules*, 64, 334–  
544 340. <http://doi.org/10.1016/j.ijbiomac.2013.11.041>

545 Acton, Q. A. (2012). *Advances in Nanotechnology Research and Application: 2012 Edition*.  
546 ScholarlyEditions. Retrieved from <https://books.google.ie/books?id=jYeUaTkR9P8C>

547 Bajaj, S., Singla, D., & Sakhuja, N. (2012). Stability testing of pharmaceutical products.  
548 *Journal of Applied Pharmaceutical Science*, 2(3), 129–138.  
549 <http://doi.org/10.7324/JAPS.2012.2322>

550 Bajpai, J., & Maan, G. K. (2012). Preparation , Characterization and Water Uptake Behavior  
551 of Polysaccharide Based Nanoparticles Swelling behavior of nanoparticles. *Progresses*  
552 *in Nanotechnology and Nanomaterials*, 1(1), 9–17.

553 Berilyn, P., So, T., Rubio, P., Lirio, S., Macabeo, A. P., Huang, H.-Y., ... Villaflores, O. B.  
554 (2016). In&nbsp;vitro angiotensin I converting enzyme inhibition by a peptide isolated  
555 from *Chiropsalmus quadrigatus* Haeckel (box jellyfish) venom hydrolysate. *Toxicon* :  
556 *Official Journal of the International Society on Toxinology*, 119, 77–83.  
557 <http://doi.org/10.1016/j.toxicon.2016.04.050>

558 Bezerra, M. A., Santelli, R. E., Oliveira, E. P., Villar, L. S., & Escaleira, L. a. (2008).  
559 Response surface methodology (RSM) as a tool for optimization in analytical chemistry.  
560 *Talanta*, 76(5), 965–977. <http://doi.org/10.1016/j.talanta.2008.05.019>

561 Bougatef, A., Nedjar-Arroume, N., Ravallec-Plé, R., Leroy, Y., Guillochon, D., Barkia, A., &  
562 Nasri, M. (2008). Angiotensin I-converting enzyme (ACE) inhibitory activities of  
563 sardinelle (*Sardinella aurita*) by-products protein hydrolysates obtained by treatment  
564 with microbial and visceral fish serine proteases. *Food Chemistry*, *111*(2), 350–356.  
565 <http://doi.org/10.1016/j.foodchem.2008.03.074>

566 Braithwaite, M. C., Tyagi, C., Tomar, L. K., Kumar, P., Choonara, Y. E., & Pillay, V. (2014).  
567 Nutraceutical-based therapeutics and formulation strategies augmenting their efficiency  
568 to complement modern medicine: An overview. *Journal of Functional Foods*.  
569 <http://doi.org/10.1016/j.jff.2013.09.022>

570 Brauner, N., & Shacham, M. (1997). Statistical analysis of linear and nonlinear correlation of  
571 the Arrhenius equation constants. *Chemical Engineering and Processing: Process*  
572 *Intensification*, *36*(3), 243–249. [http://doi.org/10.1016/S0255-2701\(96\)04186-4](http://doi.org/10.1016/S0255-2701(96)04186-4)

573 Brayden, D. J., Gleeson, J., & Walsh, E. G. (2014). A head-to-head multi-parametric high  
574 content analysis of a series of medium chain fatty acid intestinal permeation enhancers  
575 in Caco-2 cells. *European Journal of Pharmaceutics and Biopharmaceutics*, *88*(3), 830–  
576 839. <http://doi.org/10.1016/j.ejpb.2014.10.008>

577 British Pharmacopoeia Commission. (2016). *British Pharmacopoeia: Appendix XII B.*  
578 *Dissolution*. London: TSO.

579 Bruno, B. J., Miller, G. D., & Lim, C. S. (2013). Basics and recent advances in peptide and  
580 protein drug delivery. *Therapeutic Delivery*, *4*(11), 1443–67.  
581 <http://doi.org/10.4155/tde.13.104>

582 Calderon L., Harris, R., Cordoba-Diaz, M., Elorza, M., Elorza, B., Lenoir, J., ... Cordoba-  
583 Diaz, D. (2013). Nano and microparticulate chitosan-based systems for antiviral topical

584 delivery. *European Journal of Pharmaceutical Sciences*, 48, 216–222.  
585 <http://doi.org/10.1016/j.ejps.2012.11.002>

586 Calvo, P., Remu, C., Pez, N.-L., Vila-Jato, J. L., & Alonso, M. J. (1997). Novel Hydrophilic  
587 Chitosan–Polyethylene Oxide Nanoparticles as Protein Carriers. *Journal of Applied*  
588 *Polymer Science*, 63(1), 125–132. [http://doi.org/10.1002/\(SICI\)1097-](http://doi.org/10.1002/(SICI)1097-)  
589 4628(19970103)63:1<125::AID-APP13>3.0.CO;2-4

590 Calvo, P., Remunan-Lopez, C., Vila-Jato, J. L., & Alonso, M. J. (1997). Novel hydrophilic  
591 chitosan-polyethylene oxide nanoparticles as protein carriers. *Journal of Applied*  
592 *Polymer Science*, 63(1), 125–132.

593 Casey, A., Herzog, E., Davoren, M., Lyng, F. M., Byrne, H. J., & Chambers, G. (2007).  
594 Spectroscopic analysis confirms the interactions between single walled carbon  
595 nanotubes and various dyes commonly used to assess cytotoxicity. *Carbon*, 45(7), 1425–  
596 1432. <http://doi.org/10.1016/j.carbon.2007.03.033>

597 Choonara, B. F., Choonara, Y. E., Kumar, P., Bijukumar, D., du Toit, L. C., & Pillay, V.  
598 (2014). A review of advanced oral drug delivery technologies facilitating the protection  
599 and absorption of protein and peptide molecules. *Biotechnology Advances*, 32(7), 1269–  
600 1282. <http://doi.org/10.1016/j.biotechadv.2014.07.006>

601 Chuah, A. M., Kuroiwa, T., Ichikawa, S., Kobayashi, I., & Nakajima, M. (2009). Formation  
602 of biocompatible nanoparticles via the self-assembly of chitosan and modified lecithin.  
603 *Journal of Food Science*, 74(1). <http://doi.org/10.1111/j.1750-3841.2008.00985.x>

604 de Moura, M. R., Aouada, F. A., Avena-Bustillos, R. J., McHugh, T. H., Krochta, J. M., &  
605 Mattoso, L. H. C. (2009). Improved barrier and mechanical properties of novel  
606 hydroxypropyl methylcellulose edible films with chitosan/tripolyphosphate



607 nanoparticles. *Journal of Food Engineering*, 92(4), 448–453.  
608 <http://doi.org/10.1016/j.jfoodeng.2008.12.015>

609 de Pinho Neves, A. L., Milioli, C. C., Müller, L., Riella, H. G., Kuhnen, N. C., & Stulzer, H.  
610 K. (2014). Factorial design as tool in chitosan nanoparticles development by ionic  
611 gelation technique. *Colloids and Surfaces A: Physicochemical and Engineering Aspects*,  
612 445(2014), 34–39. <http://doi.org/10.1016/j.colsurfa.2013.12.058>

613 des Rieux, A., Fievez, V., Garinot, M., Schneider, Y. J., & Pr at, V. (2006). Nanoparticles as  
614 potential oral delivery systems of proteins and vaccines: A mechanistic approach.  
615 *Journal of Controlled Release*. <http://doi.org/10.1016/j.jconrel.2006.08.013>

616 Franca, E. F., Freitas, L. C. G., & Lins, R. D. (2011). Chitosan molecular structure as a  
617 function of N-acetylation. *Biopolymers*, 95(7), 448–460.  
618 <http://doi.org/10.1002/bip.21602>

619 Fu, Y., & Kao, W. J. (2009). Drug release kinetics and transport mechanisms from semi-  
620 interpenetrating networks of gelatin and poly(ethylene glycol) diacrylate.  
621 *Pharmaceutical Research*, 26(9), 2115–2124. <http://doi.org/10.1007/s11095-009-9923-1>

622 Fujita, H., & Yoshikawa, M. (1999a). LKPNM: A prodrug-type ACE-inhibitory peptide  
623 derived from fish protein. *Immunopharmacology*, 44(1–2), 123–127.  
624 [http://doi.org/10.1016/S0162-3109\(99\)00118-6](http://doi.org/10.1016/S0162-3109(99)00118-6)

625 Fujita, Yokoyama, Yoshikawa, M., Iroyukifujita, H., & Eiichiyokoyama, K. (2000).  
626 Classification and Antihypertensive Activity of Angiotensin I-Converting Enzyme  
627 Inhibitory Peptides Derived from Food Proteins. *Journal of Food Science*, 65(4), 564–  
628 569. <http://doi.org/10.1111/j.1365-2621.2000.tb16049.x>

629 Fujita, & Yoshikawa, M. (1999b). LKPNM: A prodrug-type ACE-inhibitory peptide derived  
630 from fish protein. *Immunopharmacology*, *44*(1–2), 123–127.  
631 [http://doi.org/10.1016/S0162-3109\(99\)00118-6](http://doi.org/10.1016/S0162-3109(99)00118-6)

632 García, M., Forbe, T., & Gonzalez, E. (2010). Potential applications of nanotechnology in the  
633 agro-food sector. *Ciência E Tecnologia de Alimentos*, *30*(3), 573–581.  
634 <http://doi.org/10.1590/S0101-20612010000300002>

635 Gleeson, J. P., Heade, J., Ryan, S. M. M., & Brayden, D. J. (2015). Stability, toxicity and  
636 intestinal permeation enhancement of two food-derived antihypertensive tripeptides, Ile-  
637 Pro-Pro and Leu-Lys-Pro. *TL - 71. Peptides*, *71* VN-r, 1–7.  
638 <http://doi.org/10.1016/j.peptides.2015.05.009>

639 Haung, Y., Cai, Y., & Lapitsky, Y. (2015). Factors Affecting the Stability of  
640 Chitosan/Tripolyphosphate Micro- and Nanogels: Resolving the Opposing Findings. *J.*  
641 *Mater. Chem. B*, *3*, 5957–5970. <http://doi.org/10.1039/C5TB00431D>

642 Henda, Y. Ben, Labidi, A., Arnaudin, I., Bridiau, N., Delatouche, R., Maugard, T., ...  
643 Bordenave-Juchereau, S. (2013). Measuring angiotensin-I converting enzyme inhibitory  
644 activity by micro plate assays: Comparison using marine cryptides and tentative  
645 threshold determinations with captopril and losartan. *Journal of Agricultural and Food*  
646 *Chemistry*, *61*, 10685–10690. <http://doi.org/10.1021/jf403004e>

647 Henriksson, G., Englund, A.-K., Johansson, G., & Lundahl, P. (1995). Calculation of the  
648 isoelectric points of native proteins with spreading of pKa values. *Electrophoresis*,  
649 *16*(1), 1377–1380. <http://doi.org/10.1002/elps.11501601227>

650 Hosseini, S. F., Zandi, M., Rezaei, M., & Farahmandghavi, F. (2013). Two-step method for  
651 encapsulation of oregano essential oil in chitosan nanoparticles: Preparation,

652 characterization and in vitro release study. *Carbohydrate Polymers*, 95(1), 50–56.  
653 <http://doi.org/10.1016/j.carbpol.2013.02.031>

654 Hosseinzadeh, H., Atyabi, F., Dinarvand, R., & Ostad, S. N. (2012). Chitosan-Pluronic  
655 nanoparticles as oral delivery of anticancer gemcitabine: Preparation and in vitro study.  
656 *International Journal of Nanomedicine*, 7, 1851–1863.  
657 <http://doi.org/10.2147/IJN.S26365>

658 Jarudilokkul, S., Tongthammachat, A., & Boonamnuayvittaya, V. (2011). Preparation of  
659 chitosan nanoparticles for encapsulation and release of protein. *Korean Journal of*  
660 *Chemical Engineering*, 28(5), 1247–1251. <http://doi.org/10.1007/s11814-010-0485-z>

661 Jonassen, H., Kjørniksen, A. L., & Hiorth, M. (2012). Stability of chitosan nanoparticles  
662 cross-linked with tripolyphosphate. *Biomacromolecules*, 13(11), 3747–3756.  
663 <http://doi.org/10.1021/bm301207a>

664 Lahogue, V., Réhel, K., Taupin, L., Haras, D., & Allaume, P. (2010). A HPLC-UV method  
665 for the determination of angiotensin I-converting enzyme (ACE) inhibitory activity.  
666 *Food Chemistry*, 118(3), 870–875. <http://doi.org/10.1016/j.foodchem.2009.05.080>

667 Lakshmi, P., & Kumar, G. A. (2010). Nanosuspension technology: A review. *International*  
668 *Journal of Pharmacy and Pharmaceutical Sciences*.  
669 <http://doi.org/10.2174/0929866521666140807114240>

670 Li, Y., Sadiq, F., Fu, L., Zhu, H., Zhong, M., & Sohail, M. (2016). Identification of  
671 Angiotensin I-Converting Enzyme Inhibitory Peptides Derived from Enzymatic  
672 Hydrolysates of Razor Clam *Sinonovacula constricta*. *Marine Drugs*, 14(6), 110.  
673 <http://doi.org/10.3390/md14060110>

674 López-León, T., Carvalho, E. L. S., Seijo, B., Ortega-Vinuesa, J. L., & Bastos-González, D.  
675 (2005). Physicochemical characterization of chitosan nanoparticles: electrokinetic and  
676 stability behavior. *Journal of Colloid and Interface Science*, 283(2), 344–351.  
677 <http://doi.org/10.1016/j.jcis.2004.08.186>

678 Luo, Y., Zhang, B., Cheng, W. H., & Wang, Q. (2010). Preparation, characterization and  
679 evaluation of selenite-loaded chitosan/TPP nanoparticles with or without zein coating.  
680 *Carbohydrate Polymers*, 82(3), 942–951. <http://doi.org/10.1016/j.carbpol.2010.06.029>

681 Ma, G. (2014). Microencapsulation of protein drugs for drug delivery: Strategy, preparation,  
682 and applications. *Journal of Controlled Release*, 193, 324–340.  
683 <http://doi.org/10.1016/j.jconrel.2014.09.003>

684 Madureira, A. R., Pereira, A., & Pintado, M. (2016). Chitosan nanoparticles loaded with 2,5-  
685 dihydroxybenzoic acid and protocatechuic acid: Properties and digestion. *Journal of*  
686 *Food Engineering*, 174, 8–14. <http://doi.org/10.1016/j.jfoodeng.2015.11.007>

687 Mohammadpour Dounighi, N., Eskandari, R., Avadi, M. R., Zolfagharian, H., Mir  
688 Mohammad Sadeghi, A., & Rezayat, M. (2012). Preparation and in vitro  
689 characterization of chitosan nanoparticles containing Mesobuthus eupeus scorpion  
690 venom as an antigen delivery system. *Journal of Venomous Animals and Toxins*  
691 *Including Tropical Diseases*, 18(1), 44–52. Retrieved from  
692 [http://www.scopus.com/inward/record.url?eid=2-s2.0-](http://www.scopus.com/inward/record.url?eid=2-s2.0-84859077437&partnerID=40&md5=781a81bf61973593aac773cb8b03e495)  
693 [84859077437&partnerID=40&md5=781a81bf61973593aac773cb8b03e495](http://www.scopus.com/inward/record.url?eid=2-s2.0-84859077437&partnerID=40&md5=781a81bf61973593aac773cb8b03e495)

694 Nallamuthu, I., Devi, A., & Khanum, F. (2015). Chlorogenic acid loaded chitosan  
695 nanoparticles with sustained release property, retained antioxidant activity and enhanced  
696 bioavailability. *Asian Journal of Pharmaceutical Sciences*, 10(3), 203–211.

697 <http://doi.org/10.1016/j.ajps.2014.09.005>

698 Neves, A. R., Martins, S., Segundo, M. A., & Reis, S. (2016). Nanoscale delivery of  
699 resveratrol towards enhancement of supplements and nutraceuticals. *Nutrients*, 8(3), 1–  
700 14. <http://doi.org/10.3390/nu8030131>

701 Patel, A., Patel, M., Yang, X., & Mitra, A. K. (2014). Recent advances in protein and peptide  
702 drug delivery: a special emphasis on polymeric nanoparticles. *Protein and Peptide*  
703 *Letters*, 21(11), 1102.

704 Quiñones, M., Margalef, M., Arola-Arnal, A., Muguera, B., Miguel, M., & Aleixandre, A.  
705 (2015). The blood pressure effect and related plasma levels of flavan-3-ols in  
706 spontaneously hypertensive rats. *Food & Function*, 6(11), 3479–89.  
707 <http://doi.org/10.1039/c5fo00547g>

708 R Core Team. (2015). R: A language and environment for statistical computing. R  
709 Foundation for Statistical Computing. Austria, Vienna: R Foundation for Statistical  
710 Computing,. Retrieved from <http://www.r-project.org/>

711 Rajam, M., Pulavendran, S., Rose, C., & Mandal, A. B. (2011). Chitosan nanoparticles as a  
712 dual growth factor delivery system for tissue engineering applications. *International*  
713 *Journal of Pharmaceutics*, 410(1–2), 145–152.  
714 <http://doi.org/10.1016/j.ijpharm.2011.02.065>

715 Rauk, A. P., Guo, K., Hu, Y., Cahya, S., & Weiss, W. F. (2014). Arrhenius time-scaled least  
716 squares: a simple, robust approach to accelerated stability data analysis for bioproducts.  
717 *Journal of Pharmaceutical Sciences*, 103(8), 2278–86. <http://doi.org/10.1002/jps.24063>

718 Rinaudo, M. (2006). Chitin and chitosan: Properties and applications. *Progress in Polymer*

719 *Science*, 31(7), 603–632. <http://doi.org/10.1016/j.progpolymsci.2006.06.001>

720 Ryan, S. M., McMorrow, J., Umerska, A., Patel, H. B., Kornerup, K. N., Tajber, L., ...  
721 Brayden, D. J. (2013). An intra-articular salmon calcitonin-based nanocomplex reduces  
722 experimental inflammatory arthritis. *Journal of Controlled Release*, 167(2), 120–129.  
723 <http://doi.org/10.1016/j.jconrel.2013.01.027>

724 Segura-Campos, M., Chel-Guerrero, L., Betancur-Ancona, D., & Hernandez-Escalante, V.  
725 M. (2011). Bioavailability of Bioactive Peptides. *Food Reviews International*, 27(3),  
726 213–226. <http://doi.org/10.1080/87559129.2011.563395>

727 Sharpe, L. A., Daily, A. M., Horava, S. D., & Peppas, N. A. (2014). Therapeutic applications  
728 of hydrogels in oral drug delivery. *Expert Opinion on Drug Delivery*, 11(6), 901–15.  
729 <http://doi.org/10.1517/17425247.2014.902047>

730 Siepmann, J., & Göpferich, A. (2001). Mathematical modeling of bioerodible, polymeric  
731 drug delivery systems. *Advanced Drug Delivery Reviews*, 48(2–3), 229–247.  
732 [http://doi.org/10.1016/S0169-409X\(01\)00116-8](http://doi.org/10.1016/S0169-409X(01)00116-8)

733 Silva, N. C., Silva, S., Sarmiento, B., & Pintado, M. (2013). Chitosan nanoparticles for  
734 daptomycin delivery in ocular treatment of bacterial endophthalmitis. *Drug Delivery*,  
735 7544, 1–9. <http://doi.org/10.3109/10717544.2013.858195>

736 Singh, M. R., Singh, D., Saraf, S., & Saraf, S. (2011). Formulation optimization of controlled  
737 delivery system for antihypertensive peptide using response surface methodology. *Am J*  
738 *Drug Discov Dev*, 1(3), 174–187. <http://doi.org/10.3923/ajdd.2011.174.187>

739 Sureshkumar, M. K., Das, D., Mallia, M. B., & Gupta, P. C. (2010). Adsorption of uranium  
740 from aqueous solution using chitosan-tripolyphosphate (CTPP) beads. *Journal of*

741 *Hazardous Materials*, 184(1–3), 65–72. <http://doi.org/10.1016/j.jhazmat.2010.07.119>

742 Takahashi, M., Uechi, S., Takara, K., Asikin, Y., & Wada, K. (2009). Evaluation of an Oral  
743 Carrier System in Rats: Bioavailability and Antioxidant Properties of Liposome-  
744 Encapsulated Curcumin. *Journal of Agricultural and Food Chemistry*, 57(19), 9141–  
745 9146. <http://doi.org/10.1021/jf9013923>

746 Vimal, S., Abdul Majeed, S., Taju, G., Nambi, K. S. N., Sundar Raj, N., Madan, N., ... Sahul  
747 Hameed, A. S. (2013). Chitosan tripolyphosphate (CS/TPP) nanoparticles: preparation,  
748 characterization and application for gene delivery in shrimp. *Acta Tropica*, 128(3), 486–  
749 93. <http://doi.org/10.1016/j.actatropica.2013.07.013>

750 Waterman, K. C., & Adami, R. C. (2005). Accelerated aging: Prediction of chemical stability  
751 of pharmaceuticals. *International Journal of Pharmaceutics*, 293(1–2), 101–125.  
752 <http://doi.org/10.1016/j.ijpharm.2004.12.013>

753 Weber, C., Coester, C., Kreuter, J., & Langer, K. (2000). Desolvation process and surface  
754 characterisation of protein nanoparticles. *International Journal of Pharmaceutics*,  
755 194(1), 91–102. [http://doi.org/10.1016/S0378-5173\(99\)00370-1](http://doi.org/10.1016/S0378-5173(99)00370-1)

756 Woranuch, S., & Yoksan, R. (2013). Eugenol-loaded chitosan nanoparticles: I. Thermal  
757 stability improvement of eugenol through encapsulation. *Carbohydrate Polymers*, 96(2),  
758 578–85. <http://doi.org/10.1016/j.carbpol.2012.08.117>

759 Yamaguchi, N., Kawaguchi, K., & Yamamoto, N. (2009). Study of the mechanism of  
760 antihypertensive peptides VPP and IPP in spontaneously hypertensive rats by DNA  
761 microarray analysis. *European Journal of Pharmacology*, 620(1–3), 71–77.  
762 <http://doi.org/10.1016/j.ejphar.2009.08.005>

763 Yao, M., McClements, D. J., & Xiao, H. (2015). Improving oral bioavailability of  
764 nutraceuticals by engineered nanoparticle-based delivery systems. *Current Opinion in*  
765 *Food Science*, 2, 14–19. <http://doi.org/10.1016/j.cofs.2014.12.005>

766 Yoon, H. Y., Son, S., Lee, S. J., You, D. G., Yhee, J. Y., Park, J. H., ... Pomper, M. G.  
767 (2014). Glycol chitosan nanoparticles as specialized cancer therapeutic vehicles:  
768 Sequential delivery of doxorubicin and Bcl-2 siRNA. *Scientific Reports*, 4, 6878.  
769 <http://doi.org/10.1038/srep06878>

770 Zhou, M., Du, K., Ji, P., & Feng, W. (2012). Molecular mechanism of the interactions  
771 between inhibitory tripeptides and angiotensin-converting enzyme. *Biophysical*  
772 *Chemistry*, 168–169, 60–66. <http://doi.org/10.1016/j.bpc.2012.05.002>

773



## Supplementary Material

**S1:** Fitted results of 3rd order polynomial regression against the PDI, ZP, AE % and particle size for LKP-loaded NPs

<b>Polynomial regression equation:</b> $a + b\text{Ratio} + c\text{Ratio}^2 + d\text{Ratio}^3$	<b>Coefficient of determination (<math>R^2</math>)</b>
<b>Size (nm)</b> a= - 284.90 c= - 64.68 b= 293.40 d= 4.51	$R^2 = 85.6\%$
<b>PDI</b> a = 2.31 c = 0.12 b= - 0.88 d = 0.01	$R^2 = 83.2\%$
<b>ZP (mV)</b> a = - 16.80 c = - 6.36 b = 31.05 d = 0.42	$R^2 = 76.1\%$
<b>AE (%)</b> a = 335.60 c = 43.79 b = - 202.40 d = - 2.90	$R^2 = 50.2\%$

**S2:** Loading capacities of LKP-loaded NPs, n=3

Sample	CL113 (mg/ml)	TPP (mg/ml)	Ratio (CL113/TPP)	LC %
1	1.64	0.21	8.0	2.2±0.01
2	1.52	0.33	4.5	3.3±0.00
3	1.58	0.27	5.9	2.3±0.08
4	1.45	0.40	3.6	2.7±0.03

5	1.39	0.46	3.0	2.8±0.02
---	------	------	-----	----------